

Discovery of a Potent and Selective Covalent Inhibitor and Activity-Based Probe for the Deubiquitylating Enzyme UCHL1, with Antifibrotic Activity

Nattawadee Panyain, Aurélien Godinat, Thomas Lanyon-Hogg, Sofía Lachiondo-Ortega, Edward J. Will, Christelle Soudy, Milon Mondal, Katie Mason, Sarah Elkhalfifa, Lisa M. Smith, Jeanine A. Harrigan, and Edward W. Tate*



Cite This: *J. Am. Chem. Soc.* 2020, 142, 12020–12026



Read Online

ACCESS |



Metrics & More



Article Recommendations



Supporting Information

ABSTRACT: Ubiquitin carboxy-terminal hydrolase L1 (UCHL1) is a deubiquitylating enzyme that is proposed as a potential therapeutic target in neurodegeneration, cancer, and liver and lung fibrosis. Herein we report the discovery of the most potent and selective UCHL1 probe (IMP-1710) to date based on a covalent inhibitor scaffold and apply this probe to identify and quantify target proteins in intact human cells. IMP-1710 stereoselectively labels the catalytic cysteine of UCHL1 at low nanomolar concentration in cells. We further demonstrate that potent and selective UCHL1 inhibitors block pro-fibrotic responses in a cellular model of idiopathic pulmonary fibrosis, supporting the potential of UCHL1 as a potential therapeutic target in fibrotic diseases.

Targeting the ubiquitin (Ub) proteasome system is an emerging therapeutic strategy, and deubiquitylating enzymes (DUBs) have attracted increasing interest as drug targets.¹ To study DUB biology and inhibition, Ub-derived activity-based probes (ABPs) have been developed that covalently bind to DUB active sites, allowing isolation or profiling in cell lysates.² However, they are not selective between DUBs and limited to cell-free applications, highlighting a need for complementary small-molecule ABPs to profile DUB activity in intact cells.^{3,4}

Ubiquitin carboxy-terminal hydrolase L1 (UCHL1) belongs to the UCH protease family, which feature a characteristic Cys-His-Asp catalytic triad.⁵ Although its biological functions are not yet fully understood, UCHL1 is abundantly expressed in the brain, where it is involved in apoptosis regulation, learning, and memory, while UCHL1 dysregulation is linked to diseases including neurodegeneration,⁵ cancers,^{6–8} and fibrosis.⁹

A screening and hit optimization campaign by Mission Therapeutics identified a series of novel cyanamide-containing UCHL1 inhibitors.¹⁰ Recognizing the potential of these inhibitors as covalent probes for UCHL1, we selected a potent example (**1**; example 27 in ref 10) and designed analogue IMP-1710 (**2**) bearing an alkyne tag strategically placed in line with established structure–activity relationships (Figure 1a),¹⁰ enabling functionalization and analysis postinhibition with “capture” reagents via copper(I)-catalyzed azide–alkyne cycloaddition (CuAAC).^{11,12}

We first examined biochemical UCHL1 inhibition in a fluorescence polarization (FP) assay using Ub-Lys-TAMRA.¹³ Compound **2** showed improved UCHL1 inhibition (IC₅₀ 38 nM, 95% CI 32–45 nM) over parent compound **1** (IC₅₀ 90 nM, 95% CI 79–100 nM), following 30 min of preincubation. However, the (*R*)-enantiomer of **1** (IMP-1711, **3**) was >1000-fold less active than **1**, demonstrating a highly stereoselective

interaction with UCHL1 and providing a useful negative control (Figures 1a and S1). We further characterized inhibition kinetics for **1** ($k_{\text{obs}}/I = 7400 \text{ M}^{-1} \text{ s}^{-1}$, 95% CI 5200–9700) and **2** ($k_{\text{obs}}/I = 11000 \text{ M}^{-1} \text{ s}^{-1}$, 95% CI 7700–13 000 $\text{M}^{-1} \text{ s}^{-1}$); slow recovery of activity following dilution demonstrated these inhibitors are slowly reversible (Figure S2), in line with previous reports on cyanamide warheads.¹⁴ Cross-screening against 20 DUBs demonstrated exquisite selectivity for **1** and **2** for UCHL1 (Figure 1b), whereas control compound **3** was inactive against all tested DUBs (Figure S1). Cellular UCHL1 activity was demonstrated in breast cancer cells (Cal51) stably expressing FLAG-UCHL1 using a Ub-vinyl methyl ester probe (HA-Ub-VME) by a homogeneous time-resolved fluorescence (HTRF) assay.¹⁵ Compounds **1** and **2** engaged UCHL1 with an in-cell IC₅₀ of 820 and 110 nM, respectively (Figure S3). Selective in-cell concentration-dependent competition by **1** and **2** for UCHL1 was confirmed through immunoblot analysis against HA-Ub-VME labeling (Figures 1c and S4). Cellular potencies were in line with biochemical data (Figure S1), and compound **3** did not inhibit UCHL1 in cells.

We next compared our probes to the most potent known UCHL1 inhibitor, isatin *O*-acyloxime LDN-57444 (Figure 1a), reported as a reversible Ub-competitive UCHL1 inhibitor with IC₅₀ 880 nM against recombinant UCHL1¹⁶ and widely used as a tool inhibitor in UCHL1 studies in disease models.^{7,9,17,18} However, engagement of UCHL1 in intact cells has not

Received: May 5, 2020

Published: June 24, 2020



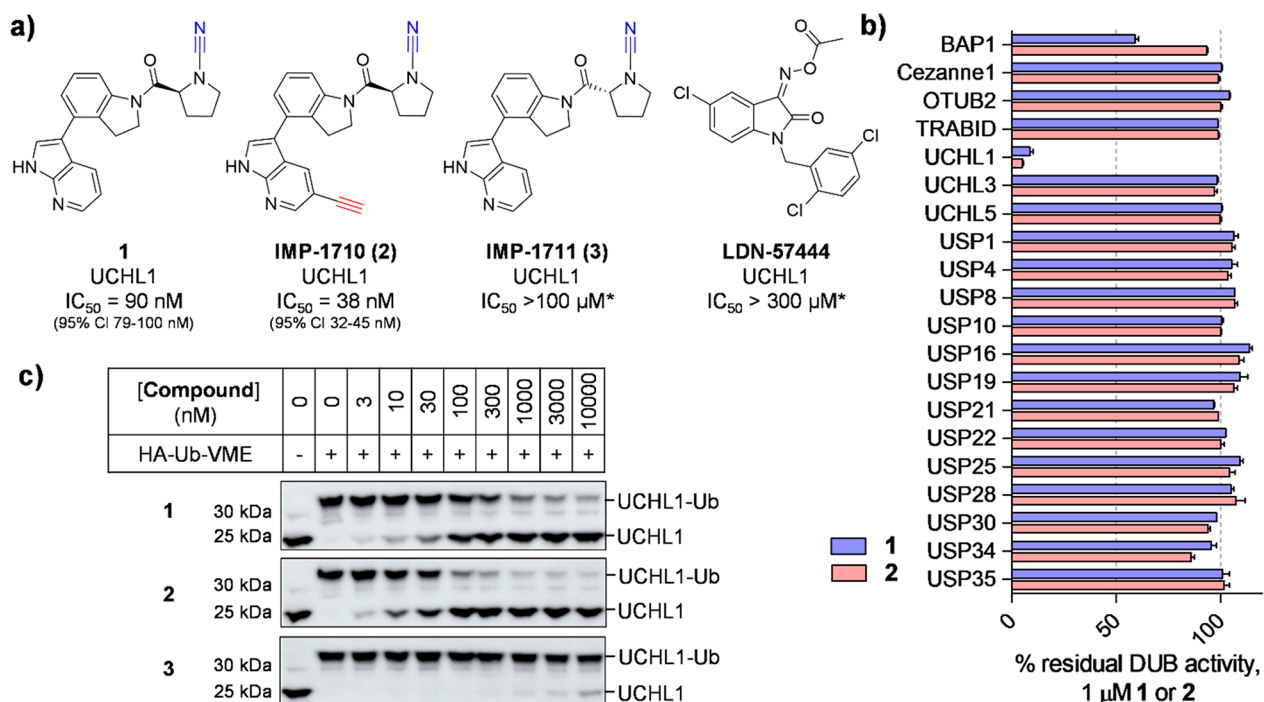


Figure 1. Potency and selectivity of UCHL1 inhibitor (1), alkyne ABP (IMP-1710, 2), control compound (IMP-1711, 3), and LDN-57444. (a) Structures and UCHL1 IC_{50} values (Ub-Lys-TAMRA FP assay; *maximum assay concentration). (b) Selectivity profiling of 1 and 2 against DUBs in FP and FI assays (Ub-Lys-TAMRA and Ub-Rho110, respectively). See Supporting Information for 3 and LDN-57444 profiling. Data represent mean \pm SEM ($n = 2$). (c) Immunoblot analysis of HA-Ub-VME UCHL1 labeling following HEK293T treatment with 1, 2, or 3 for 1 h. Dose-dependent competition for UCHL1 labeling occurs for active compounds, but not inactive enantiomer 3.

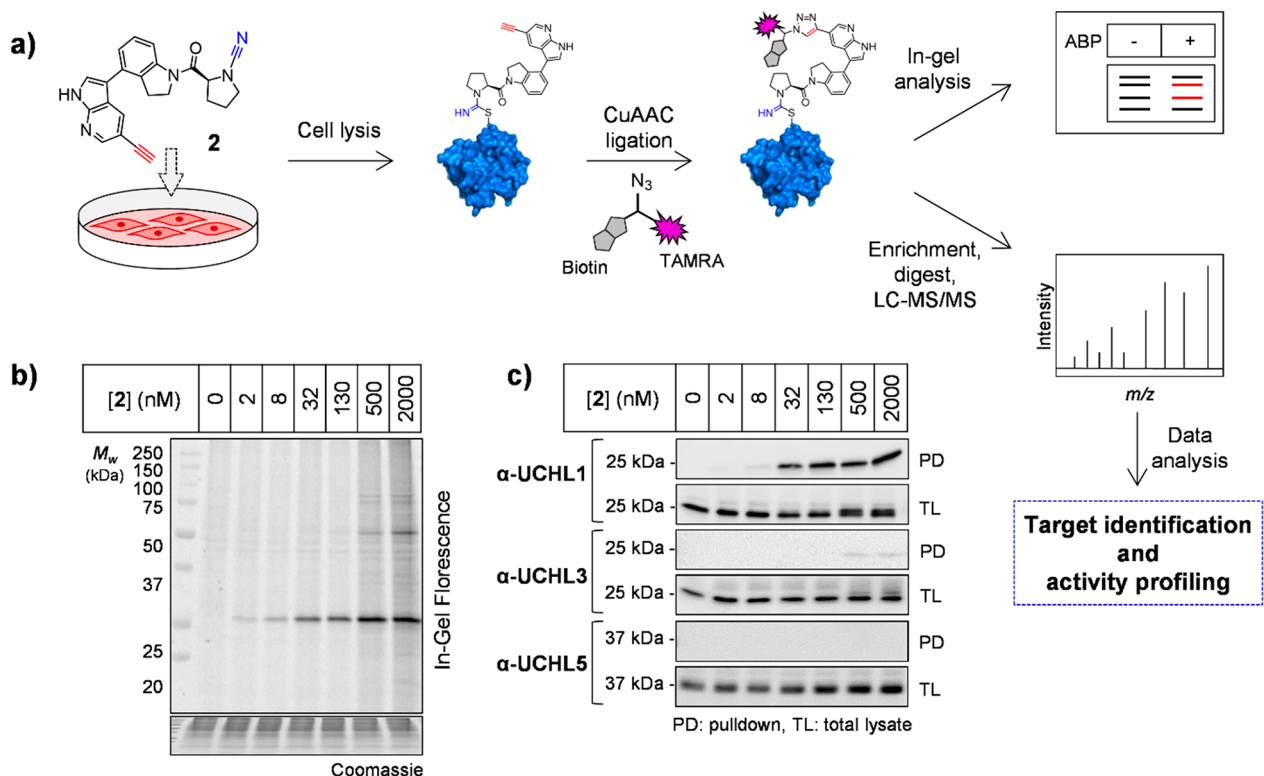


Figure 2. UCHL1 activity profiling using ABP 2 in HEK293 cells. (a) Chemical proteomics workflow. Cells were incubated with 2 and labeled proteins ligated via CuAAC to AzTB for in-gel fluorescence and/or affinity enrichment for immunoblotting and proteomic profiling. (b) In-gel fluorescence shows dose-dependent labeling by 2. (c) Probe-labeled protein identification by enrichment and immunoblotting.

previously been demonstrated, and we were surprised to discover that LDN-57444 failed to engage UCHL1 in a range

of assays, including biochemical activity and capacity to bind UCHL1 in intact cells (Figures S1, S3, S4).

Direct target engagement by **2** was examined in HEK293 cells treated for 60 min, followed by lysis and CuAAC ligation to azide-TAMRA-biotin capture reagent (AzTB, Figure S5) (Figure 2a).¹¹ In-gel fluorescence revealed one major target at ~25 kDa labeled in a concentration-dependent manner and saturated at 130 nM **2**, with some off-target labeling of >500 nM (Figure 2b). Labeling was confirmed by biotin pull-down and immunoblotting, with UCHL1 significantly enriched at 30 nM **2** and maximal at 130 nM, with minimal or no detectable labeling of UCHL3, UCHL5, and DUBs from other families (Figures 2c and S6). Time course experiments demonstrated maximal labeling within 60 min (Figure S7), and **2** remained stable in media for >72 h without loss of activity (Figure S8). Incubation of recombinant UCHL1 (5 μ M) with **1** or **2** (13 μ M) for 60 min led to single modification of UCHL1 by LC-ESI-MS (Figure 3a), occurring specifically at the catalytic cysteine (Cys90) by

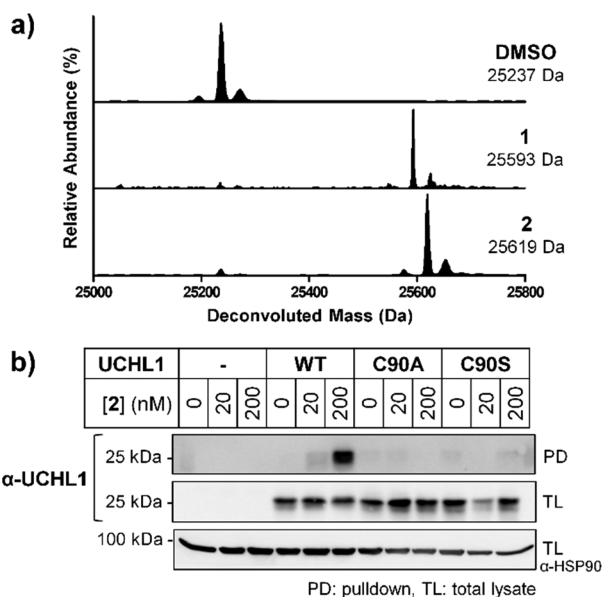


Figure 3. UCHL1 labeling with **1** or **2** exclusively at catalytic Cys90 *in vitro* and in intact cells. (a) LC-ESI demonstrating single UCHL1 covalent modification with **1** or **2**. (b) HeLa cells lacking endogenous UCHL1, transfected to express UCHL1 wild-type (WT) or catalytic cysteine mutants (C90A and C90S); pull-down following treatment with **2** and AzTB functionalization confirms specific Cys90 labeling.

tryptic digest and nanoLC-MS/MS (Figure S9, Supplementary Data S1). To confirm dependence on UCHL1 catalytic activity for cellular target engagement, we overexpressed FLAG-tagged wild-type (WT) UCHL1 or C90A or C90S mutants in HeLa cells, which do not express UCHL1, and demonstrated that only WT UCHL1 is labeled by **2** (Figures 3b and S10).¹⁹ Taken together, these data demonstrate **2** is a bona fide UCHL1 ABP that rapidly targets endogenous UCHL1 in cells in a strictly activity-dependent manner.

To determine selectivity across the proteome, unbiased quantitative chemical proteomic profiling (Figure 2a) was employed in HEK293 cells treated with **2** (2, 20, or 200 nM) or vehicle (DMSO) control, for 10, 60, or 180 min. CuAAC ligation of proteins to azide-arginine-biotin (AzRB, Figure S5) capture reagent¹¹ and enrichment on dimethylated NeutrAvidin-agarose beads were followed by on-resin digestion with LysC followed by trypsin²⁰ and labeling with tandem mass tags (TMT) to enable relative quantification between conditions

following nanoLC-MS/MS analysis. UCHL1 was significantly enriched by **2** in a concentration-dependent manner, with marginal enrichment of UCHL3 at higher concentrations and no significant enrichment of any other DUB (Figures 4a and S11); UCHL1 enrichment was similar at all time points, in line with in-gel fluorescence analysis (Figure S7). Only two proteins, UCHL1 and fibroblast growth factor receptor 2 (FGFR2), were significantly enriched at 20 nM **2**, with UCHL1 by far the major target (Figure 4b, Supplementary Data S2). Full dose-response analysis by immunoblotting demonstrated that FGFR2 enrichment was barely detectable at any concentration up to 2 μ M (Figure 4c), compared to UCHL1, which was strongly enriched and reached saturation at 130 nM (Figure 2c), suggesting that FGFR2 is minimally engaged by **2** at concentrations that strongly inhibit UCHL1. No significant abundance change was detected in whole proteome analysis (Figure S12, Supplementary Data S3), suggesting that **2** does not substantially alter global protein homeostasis. In-gel fluorescence and immunoblot analysis further confirmed **2** can profile activity of endogenous UCHL1 with excellent selectivity in cell types including endothelial cells (EA.hy926) and adenocarcinoma human alveolar basal epithelial cells (A549) (Figure S13).

To identify selective targets of parent compound **1** and differentiate between selective labeling and nonspecific pull-down, competitive activity-based protein profiling (ABPP) was performed.^{21,22} HEK293 cells were treated with **1**, **3**, or LDN-57444 for 1 h, followed by **2** (20 nM) for 10 min. Immunoblot analysis demonstrated dose-dependent UCHL1 labeling reduction with parent compound **1** at nanomolar concentrations, whereas no competition was observed with control compound **3** or LDN-57444, confirming **3** as an effective negative control and LDN-57444 as inactive against UCHL1 in cells (Figure 4d and e). In-cell proteome-wide competitive ABPP was performed by quantitative chemical proteomics, showing that across the whole proteome UCHL1 responds strongly to **1** in a concentration-dependent manner, but does not respond with inactive control **3** or LDN-57444 (Figure 4f and S14, Supplementary Data S4). UCHL3 shows a small response to **1**, while outside the DUB family FGFR2 responds (Figure S14), suggesting these proteins are possible minor off-targets of **1**.

Pharmacological UCHL1 inhibition was next investigated in primary human lung cells derived from idiopathic pulmonary fibrosis (IPF) patients based on the potential of UCHL1 as a therapeutic target in fibrosis.^{9,23} Fibroblast-myofibroblast transition (FMT) was stimulated by transforming growth factor beta 1 (TGF- β 1) using alpha-smooth muscle actin (α SMA) as a disease-relevant marker for transition (Figure 5a)^{24,25} and validated by high content imaging analysis (HCA) of three donor cell lines alongside response to 1 h pretreatment with 1 μ M TGF- β 1 receptor kinase inhibitor SB525334 (Figure S15).²⁶ Donor cells were treated with compounds **1**, **2**, **3**, LDN-57444, or the FDA-approved IPF drug nintedanib,²⁷ and response to TGF- β 1 and cell viability were measured after 3 days by staining and HCA quantification of α SMA and nuclei (DAPI), respectively.

Compounds **1** and **2** (1 μ M) demonstrated >50% FMT inhibition (IC₅₀ 100 and 740 nM, respectively), with comparable potency to nintedanib (Figure 5b), and inactive control compound **3** showed minimal α SMA inhibition compared to **1** and **2**. While the dose-response observed for inhibition suggests a potentially complex role for UCHL1 in FMT, nuclear count remained stable at <5 μ M, providing a good

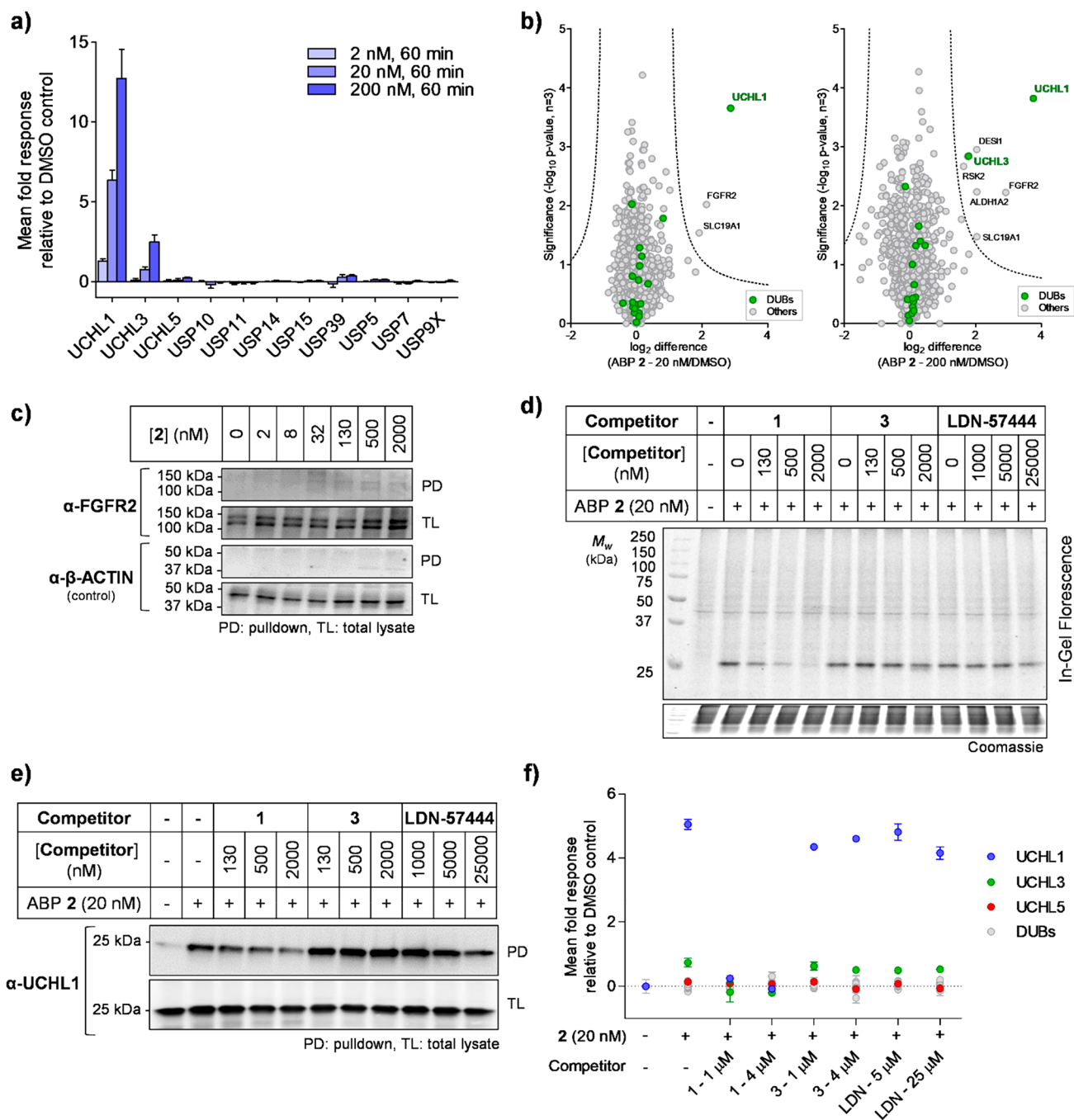


Figure 4. Chemical proteomic analysis of ABP 2 labeling in HEK293 cells. (a) Selected DUB quantitative profiling by 2, demonstrating dose-dependent enrichment of UCHL1. Data represent mean \pm SEM ($n = 3$). (b) Volcano plots showing \log_2 difference (fold change) and significance ($-\log_{10} p$ -value) between protein enrichment at 20 or 200 nM 2 compared to DMSO control (two sample t test, $n = 3$, permutation-based FDR = 0.01, $S_0 = 1$). (c) FGFR2 shows negligible enrichment by 2, as determined by pull-down and immunoblotting. (d, e, f) Compound 1 selectively competes with ABP 2, while 3 and LDN-57444 do not. Competition for ABP 2 labeling was confirmed by (d) in-gel fluorescence; (e) pull-down and UCHL1 immunoblotting; (f) pull-down and whole proteome quantitative proteomic analysis. Data represent mean \pm SEM ($n = 3$).

window between inhibition and cytotoxicity (Figure S16). Although LDN-57444 showed evidence for weak α SMA inhibition, this was concurrent with increased cytotoxicity over the same concentration range, suggesting that LDN-57444 toxicity may drive decreased α SMA (Figure S16).

In summary, we report the discovery and characterization of the most potent and selective small-molecule DUB ABP (2) to date, enabling robust detection of UCHL1 activity in living cells at low nanomolar concentrations. The only previously reported UCHL1 ABP is >150-fold less potent than 2 and has multiple

significant off-targets,¹⁴ with no selectivity over UCHL3. UCHL1 labeling by 2 is strictly activity-dependent, occurring only at the catalytic cysteine and providing a new chemical tool to examine UCHL1 activity in various intact cell types. ABPP demonstrated that parent compound 1 is a potent UCHL1 inhibitor that targets the active site cysteine residue with impressive selectivity in cells and that UCHL1 inhibition is highly stereoselective, providing an ideal control compound (3) for future studies. Further, evidence from multiple assays (biochemical, cellular, proteomics) demonstrates that LDN-

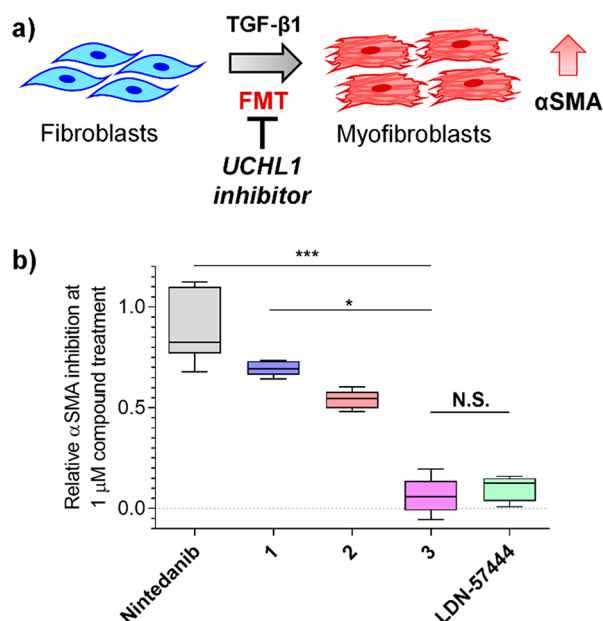


Figure 5. Phenotypic effects of selective UCHL1 inhibition in idiopathic pulmonary fibrosis (IPF). (a) Schematic of TGF- β 1-mediated fibroblast-to-myfibroblast transition in primary human lung fibroblasts, increasing alpha-smooth muscle actin (α SMA) transdifferentiation marker. (b) Primary fibroblasts from IPF donors were preincubated with 1 μ M 1, 2, 3, LDN-57444, or IPF approved drug (nintedanib) for 1 h followed by TGF- β 1 treatment for 3 days. α SMA expression was analyzed by high content imaging, demonstrating 1, 2, and nintedanib, but not 3 or LDN-57444, inhibit transdifferentiation (N.S. nonsignificant, * $P \leq 0.05$, *** $P \leq 0.01$). Plots represent median values (center lines) and 25th/75th percentiles (box limits) with Tukey whiskers.

57444 showed negligible inhibition compared to 1 and 2.^{16,28} Previous studies with multiple batches of LDN-57444 suggest that its reported biochemical activity may be assay-dependent²⁹ and further support reinterpretation of previous cellular studies using this compound. Finally, we show that selective UCHL1 inhibitors can suppress fibrotic phenotypes in IPF cellular models without substantial cytotoxicity. While the precise role of UCHL1 in fibrosis remains to be determined, UCHL1 was recently identified as a potential target in triple-negative breast cancer (TNBC), where it promotes TGF- β 1 signaling⁸ and suppresses estrogen receptor expression.³⁰ 1 and 2 represent powerful and selective probes to explore UCHL1 activity with potential application to substrate identification, mode of action studies, and cellular target profiling, which can accelerate future development of UCHL1 inhibitors as potential therapeutics.

The mass spectrometry proteomics data have been deposited to the ProteomeXchange Consortium via the PRIDE partner repository³¹ with the data set identifier PXD015825.

■ ASSOCIATED CONTENT

Supporting Information

The Supporting Information is available free of charge at <https://pubs.acs.org/doi/10.1021/jacs.0c04527>.

Additional results and materials and methods for protein production, biochemical assay, cell-based experiment, chemical proteomic sample preparation and data analysis, and FMT assay; detailed chemical synthesis for all synthesized compounds; ¹H, ¹³C NMR spectra and HRMS data (PDF)

Data files of protein identification and quantification from the proteomic experiments (ZIP)

■ AUTHOR INFORMATION

Corresponding Author

Edward W. Tate – Department of Chemistry, Molecular Sciences Research Hub, Imperial College London, London W12 0BZ, U.K.; The Francis Crick Institute, London NW1 1AT, U.K.; orcid.org/0000-0003-2213-5814; Email: e.tate@imperial.ac.uk

Authors

Nattawadee Panyain – Department of Chemistry, Molecular Sciences Research Hub, Imperial College London, London W12 0BZ, U.K.

Aurélien Godinat – Department of Chemistry, Molecular Sciences Research Hub, Imperial College London, London W12 0BZ, U.K.

Thomas Lanyon-Hogg – Department of Chemistry, Molecular Sciences Research Hub, Imperial College London, London W12 0BZ, U.K.; orcid.org/0000-0002-7092-8096

Sofia Lachiondo-Ortega – Department of Chemistry, Molecular Sciences Research Hub, Imperial College London, London W12 0BZ, U.K.

Edward J. Will – Department of Chemistry, Molecular Sciences Research Hub, Imperial College London, London W12 0BZ, U.K.; orcid.org/0000-0003-4768-692X

Christelle Soudy – The Francis Crick Institute, London NW1 1AT, U.K.

Milon Mondal – Department of Chemistry, Molecular Sciences Research Hub, Imperial College London, London W12 0BZ, U.K.

Katie Mason – Mission Therapeutics Ltd, Cambridge CB22 3AT, U.K.

Sarah Elkhalfa – Mission Therapeutics Ltd, Cambridge CB22 3AT, U.K.

Lisa M. Smith – Mission Therapeutics Ltd, Cambridge CB22 3AT, U.K.

Jeanine A. Harrigan – Mission Therapeutics Ltd, Cambridge CB22 3AT, U.K.

Complete contact information is available at: <https://pubs.acs.org/10.1021/jacs.0c04527>

Notes

The authors declare the following competing financial interest(s): K.M., S.E., L.M.S., and J.A.H. are current or previous employees of Mission Therapeutics Ltd; E.W.T. is a Director and shareholder in Myricx Pharma Ltd.

■ ACKNOWLEDGMENTS

The authors thank L. Haigh (Department of Chemistry Mass Spectrometry Facility, Imperial College London) for assistance in acquiring nanoLC-MS/MS, LC-ESI, and high-resolution mass spectrometry (HRMS) data, C. Das (Purdue University) for a UCHL1 DNA construct, M. Morgan (Imperial College London) for assistance with structural studies, D. Conole (Imperial College London) for insightful comments on the manuscript, Charles River (Leiden, Netherlands) for FMT data, and R. Williams, N. Jama, and C. Stead (Mission Therapeutics) for technical assistance. This study was supported by Cancer Research UK (Programme Foundation Award C29637/A20183 to E.W.T.), Royal Thai Government scholarship (PhD studentship to N.P.), Swiss National Science Foundation (Early Postdoc Mobility Fellowship P2ELP2_175069 to A.G.), and

the Francis Crick Institute, which receives its core funding from Cancer Research UK (FC001097, FC010636), the UK Medical Research Council (FC001097, FC010636), and the Wellcome Trust (FC001097, FC010636).

REFERENCES

- (1) Harrigan, J. A.; Jacq, X.; Martin, N. M.; Jackson, S. P. Deubiquitylating enzymes and drug discovery: emerging opportunities. *Nat. Rev. Drug Discovery* **2018**, *17* (1), 57–78.
- (2) Hewings, D. S.; Flygare, J. A.; Bogyo, M.; Wertz, I. E. Activity-based probes for the ubiquitin conjugation-deconjugation machinery: new chemistries, new tools, and new insights. *FEBS J.* **2017**, *284* (10), 1555–1576.
- (3) Ward, J. A.; McLellan, L.; Stockley, M.; Gibson, K. R.; Whitlock, G. A.; Knights, C.; Harrigan, J. A.; Jacq, X.; Tate, E. W. Quantitative Chemical Proteomic Profiling of Ubiquitin Specific Proteases in Intact Cancer Cells. *ACS Chem. Biol.* **2016**, *11* (12), 3268–3272.
- (4) Conole, D.; Mondal, M.; Majmudar, J. D.; Tate, E. W. Recent Developments in Cell Permeable Deubiquitinating Enzyme Activity-Based Probes. *Front. Chem.* **2019**, *7*, 876–882.
- (5) Bishop, P.; Rocca, D.; Henley, J. M. Ubiquitin C-terminal hydrolase L1 (UCH-L1): structure, distribution and roles in brain function and dysfunction. *Biochem. J.* **2016**, *473* (16), 2453–2462.
- (6) Hurst-Kennedy, J.; Chin, L. S.; Li, L. Ubiquitin C-terminal hydrolase 1 in tumorigenesis. *Biochem. Res. Int.* **2012**, *2012*, 123706.
- (7) Goto, Y.; Zeng, L.; Yeom, C. J.; Zhu, Y.; Morinibu, A.; Shinomiya, K.; Kobayashi, M.; Hirota, K.; Itasaka, S.; Yoshimura, M.; Tanimoto, K.; Torii, M.; Sowa, T.; Menju, T.; Sonobe, M.; Kakeya, H.; Toi, M.; Date, H.; Hammond, E. M.; Hiraoka, M.; Harada, H. UCHL1 provides diagnostic and antimetastatic strategies due to its deubiquitinating effect on HIF-1 α . *Nat. Commun.* **2015**, *6*, 6153–6165.
- (8) Liu, S.; Gonzalez-Prieto, R.; Zhang, M.; Geurink, P. P.; Kooij, R.; Iyengar, P. V.; van Dinther, M.; Bos, E.; Zhang, X.; Le Devedec, S. E.; van de Water, B.; Koning, R. I.; Zhu, H. J.; Mesker, W. E.; Vertegaal, A. C. O.; Ova, H.; Zhang, L.; Martens, J. W. M.; Ten Dijke, P. Deubiquitinase Activity Profiling Identifies UCHL1 as a Candidate Oncoprotein That Promotes TGF β -Induced Breast Cancer Metastasis. *Clin. Cancer Res.* **2020**, *26* (6), 1460–1473.
- (9) Wilson, C. L.; Murphy, L. B.; Leslie, J.; Kendrick, S.; French, J.; Fox, C. R.; Sheerin, N. S.; Fisher, A.; Robinson, J. H.; Tiniakos, D. G.; Gray, D. A.; Oakley, F.; Mann, D. A. Ubiquitin C-terminal hydrolase 1: A novel functional marker for liver myofibroblasts and a therapeutic target in chronic liver disease. *J. Hepatol.* **2015**, *63* (6), 1421–1428.
- (10) Kemp, M.; Stockley, M.; Jones, A. Cyanopyrrolidines as Dub Inhibitors for the Treatment of Cancer. WO 2017009650 (A1), 2017/01/19/, 2017.
- (11) Broncel, M.; Serwa, R. A.; Ciepla, P.; Krause, E.; Dallman, M. J.; Magee, A. I.; Tate, E. W. Multifunctional reagents for quantitative proteome-wide analysis of protein modification in human cells and dynamic profiling of protein lipidation during vertebrate development. *Angew. Chem., Int. Ed.* **2015**, *54* (20), 5948–5951.
- (12) Storck, E. M.; Morales-Sanfrutos, J.; Serwa, R. A.; Panyain, N.; Lanyon-Hogg, T.; Tolmachova, T.; Ventimiglia, L. N.; Martin-Serrano, J.; Seabra, M. C.; Wojciak-Stothard, B.; Tate, E. W. Dual chemical probes enable quantitative system-wide analysis of protein prenylation and prenylation dynamics. *Nat. Chem.* **2019**, *11* (6), 552–561.
- (13) Geurink, P. P.; El Oualid, F.; Jonker, A.; Hameed, D. S.; Ova, H. A general chemical ligation approach towards isopeptide-linked ubiquitin and ubiquitin-like assay reagents. *ChemBioChem* **2012**, *13* (2), 293–297.
- (14) Krabill, A. D.; Chen, H.; Hussain, S.; Feng, C.; Abdullah, A.; Das, C.; Aryal, U. K.; Post, C. B.; Wendt, M. K.; Galardy, P. J.; Flaherty, D. P. Ubiquitin C-Terminal Hydrolase L1: Biochemical and Cellular Characterization of a Covalent Cyanopyrrolidine-Based Inhibitor. *ChemBioChem* **2020**, *21* (5), 712–722.
- (15) Yabuki, N.; Watanabe, S.; Kudoh, T.; Nihira, S.; Miyamoto, C. Application of homogeneous time-resolved fluorescence (HTRFTM) to monitor poly-ubiquitination of wild-type p53. *Comb. Chem. High Throughput Screen* **1999**, *2* (5), 279–287.
- (16) Liu, Y.; Lashuel, H. A.; Choi, S.; Xing, X.; Case, A.; Ni, J.; Yeh, L. A.; Cuny, G. D.; Stein, R. L.; Lansbury, P. T., Jr. Discovery of inhibitors that elucidate the role of UCH-L1 activity in the H1299 lung cancer cell line. *Chem. Biol.* **2003**, *10* (9), 837–846.
- (17) Yan, C.; Huo, H.; Yang, C.; Zhang, T.; Chu, Y.; Liu, Y. Ubiquitin C-Terminal Hydrolase L1 regulates autophagy by inhibiting autophagosome formation through its deubiquitinating enzyme activity. *Biochem. Biophys. Res. Commun.* **2018**, *497* (2), 726–733.
- (18) Kobayashi, E.; Hwang, D.; Bheda-Malge, A.; Whitehurst, C. B.; Kabanov, A. V.; Kondo, S.; Aga, M.; Yoshizaki, T.; Pagano, J. S.; Sokolsky, M.; Shakelford, J. Inhibition of UCH-L1 Deubiquitinating Activity with Two Forms of LDN-57444 Has Anti-Invasive Effects in Metastatic Carcinoma Cells. *Int. J. Mol. Sci.* **2019**, *20* (15), 3733–3750.
- (19) Larsen, C. N.; Price, J. S.; Wilkinson, K. D. Substrate binding and catalysis by ubiquitin C-terminal hydrolases: identification of two active site residues. *Biochemistry* **1996**, *35* (21), 6735–6744.
- (20) Goya Grocin, A.; Serwa, R. A.; Morales Sanfrutos, J.; Ritzefeld, M.; Tate, E. W. Whole Proteome Profiling of N-Myristoyltransferase Activity and Inhibition Using Sortase A. *Mol. Cell. Proteomics* **2019**, *18* (1), 115–126.
- (21) Kalesh, K. A.; Clulow, J. A.; Tate, E. W. Target profiling of zerumbone using a novel cell-permeable clickable probe and quantitative chemical proteomics. *Chem. Commun. (Cambridge, U. K.)* **2015**, *51* (25), 5497–5500.
- (22) Clulow, J. A.; Storck, E. M.; Lanyon-Hogg, T.; Kalesh, K. A.; Jones, L. H.; Tate, E. W. Competition-based, quantitative chemical proteomics in breast cancer cells identifies new target profiles for sulforaphane. *Chem. Commun. (Cambridge, U. K.)* **2017**, *53* (37), 5182–5185.
- (23) Cheng, J. C.; Tseng, C. P.; Liao, M. H.; Peng, C. Y.; Yu, J. S.; Chuang, P. H.; Huang, J. T.; Chen, J. J. W. Activation of hepatic stellate cells by the ubiquitin C-terminal hydrolase 1 protein secreted from hepatitis C virus-infected hepatocytes. *Sci. Rep.* **2017**, *7* (1), 4448–4459.
- (24) Lepparanta, O.; Sens, C.; Salmenkivi, K.; Kinnula, V. L.; Keski-Oja, J.; Myllarniemi, M.; Koli, K. Regulation of TGF- β storage and activation in the human idiopathic pulmonary fibrosis lung. *Cell Tissue Res.* **2012**, *348* (3), 491–503.
- (25) Saito, A.; Horie, M.; Nagase, T. TGF- β Signaling in Lung Health and Disease. *Int. J. Mol. Sci.* **2018**, *19* (8), 2460–2477.
- (26) Grygielko, E. T.; Martin, W. M.; Tweed, C.; Thornton, P.; Harling, J.; Brooks, D. P.; Laping, N. J. Inhibition of gene markers of fibrosis with a novel inhibitor of transforming growth factor- β type I receptor kinase in puromycin-induced nephritis. *J. Pharmacol. Exp. Ther.* **2005**, *313* (3), 943–951.
- (27) Richeldi, L.; du Bois, R. M.; Raghu, G.; Azuma, A.; Brown, K. K.; Costabel, U.; Cottin, V.; Flaherty, K. R.; Hansell, D. M.; Inoue, Y.; Kim, D. S.; Kolb, M.; Nicholson, A. G.; Noble, P. W.; Selman, M.; Taniguchi, H.; Brun, M.; Le Maulf, F.; Girard, M.; Stowasser, S.; Schlenker-Herceg, R.; Disse, B.; Collard, H. R.; Investigators, I. T. Efficacy and safety of nintedanib in idiopathic pulmonary fibrosis. *N. Engl. J. Med.* **2014**, *370* (22), 2071–2082.
- (28) D'Arcy, P.; Wang, X.; Linder, S. Deubiquitinase inhibition as a cancer therapeutic strategy. *Pharmacol. Ther.* **2015**, *147*, 32–54.
- (29) Kemp, M. Recent Advances in the Discovery of Deubiquitinating Enzyme Inhibitors. *Prog. Med. Chem.* **2016**, *55*, 149–192.
- (30) Chen, X. S.; Wang, K. S.; Guo, W.; Li, L. Y.; Yu, P.; Sun, X. Y.; Wang, H. Y.; Guan, Y. D.; Tao, Y. G.; Ding, B. N.; Yin, M. Z.; Ren, X. C.; Zhang, Y.; Chen, C. S.; Ye, Y. C.; Yang, J. M.; Cheng, Y. UCH-L1-mediated Down-regulation of Estrogen Receptor α Contributes to Insensitivity to Endocrine Therapy for Breast Cancer. *Theranostics* **2020**, *10* (4), 1833–1848.
- (31) Vizcaino, J. A.; Deutsch, E. W.; Wang, R.; Csordas, A.; Reisinger, F.; Rios, D.; Dianes, J. A.; Sun, Z.; Farrar, T.; Bandeira, N.; Binz, P. A.; Xenarios, I.; Eisenacher, M.; Mayer, G.; Gatto, L.; Campos, A.; Chalkley, R. J.; Kraus, H. J.; Albar, J. P.; Martinez-Bartolome, S.; Apweiler, R.; Omenn, G. S.; Martens, L.; Jones, A. R.; Hermjakob, H.

ProteomeXchange provides globally coordinated proteomics data submission and dissemination. *Nat. Biotechnol.* **2014**, *32* (3), 223–226.